

# Interaction of molten secondary metallurgical ladle slag with MgO-C refractories

Anton Yehorov, TU Bergakademie Freiberg; Olena Volkova, TU Bergakademie Freiberg, Freiberg, Germany

Marcel Mix, INTOCAST AG; Natalie Froese, INTOCAST AG, Ratingen, Germany

## ABSTRACT

The present work experimentally studied the corrosion behavior of MgO-C ladle refractory exposed to molten slag during steel refining. The corrosion of ladle refractories, especially at the slag line, causes issues that require maintenance and repair and can even lead to melt outages.

## INTRODUCTION

Carbon bonded ceramics are in high demand in iron and steelmaking industries as the refractory material [1,2]. The addition of carbon into the oxides is considered as the beneficial approach to enhance its thermal properties such as thermal shock resistance, thermal conductivity, minimize the corrosion, and erosion process of the liquid slags, i.e. due to the low wettability of graphite to the liquid slags [3–5].

Magnesia-carbon refractory materials (MgO-C) is the most widespread carbon bonded ceramic for steelmaking industry. They are applied as a lining material in steel ladles, basic oxygen furnaces (BOF), electric arc (EAF) furnaces, and casting furnaces [6–8]. The service life of refractory material can vary from type steelmaking. This is strongly correlated the factors such as: temperature, pressure, atmosphere, and chemical reactivity of the melt. Changing these production conditions could enhance the carbon oxidation, the increasing of open porosity, and the dissolution of MgO grains into slag [9–11]. All of this phenomena lead to a decrease of life time of the refractory [12].

Normally, when the steel ladle is preheated above 500 °C, carbon from the MgO-C refractory material reacts with oxygen in the pores and form CO<sub>2</sub>-gas on the surface of the refractory [13].

Subsequently, as the CO<sub>2</sub> temperature rises, the CO<sub>2</sub> gas reacts further with carbon to form CO gas. This type of reaction is called direct carbon oxidation.

However, above 1400 °C an indirect carbon oxidation takes place in the MgO-C refractory. This reaction involves the reaction between MgO and carbon, found in resin and graphite, resulting in the formation of Mg and CO gases [14–17].

The oxidation process not only increases the weight loss of the refractory material, but also enhances the open porosity. Open porosity represents the effective volume of pores within the refractory that can be penetrated by melt. An increase in the open porosity of the refractory has a negative effect on the corrosion resistance of the refractory in contact with molten slags and metals. Corrosion in MgO-C can be divided into three stages [14]:

1 – The penetration of the melt into the hot surface of the refractory material. If the temperature of the refractory falls below the solidus temperature of the melt, the melt freezes and penetration stops.

2 - If the melt does not freeze, it penetrates the capillaries of the refractory. The melt penetrates the refractory material through the capillary infiltration, which affects the refractory matrix. Infiltration usually occurs when there are large temperature gradients from the hot surface to the cold surface of the refractory material.

3 - Refractory material is impregnated with melt to such an extent that the core is held together by the melt as the matrix corrodes.

According to the increased requirements, a change in the chemical composition of the steel or process leads to a change in the chemical composition of the slag. These changes directly affect the ability of the slag to dissolve the refractory, and the thermophysical properties of the slag. The penetration and infiltration of refractory material by the melt is influenced by the open porosity, wetting angle of the refractory, viscosity, surface tension, and contact time, **Equation 1**[18–21].

$$l^2 = \frac{r \cdot \sigma \cdot \cos\theta}{2\eta} \cdot t \quad \text{Equation 1}$$

where  $r$  (m) is the open pore radius of refractory,  $\sigma$  (N/m) is the surface tension of the slag,  $\theta$  is the contact angle between the slag and refractory,  $\eta$  (Pa·s) is the slag viscosity,  $t$  (s) is the contact time and  $l$  (m) is the infiltration depth.

Hence, a combination of high viscosity, low surface tension, open porosity, and appropriate contact angle serves to minimize the infiltration of slag into the refractory and subsequent dissolution [18]. Besides, temperature also has a great influence on MgO-C refractory wear, with increasing temperature, the viscosity values decrease and the maximum dissolution of MgO in the slag increases. This allows the slag to penetrate deeper into the refractory and actively dissolve its grains, weakening the entire structure.

Borges et al. studied the addition of sodium to desulphurisation slags and showed the sodium addition to calcium-aluminium silicates increases the dissolution of MgO grains and reduces the life of the steel ladle [22]. Guo et al. investigated the effect of VOD (Vacuum Oxygen Decarburization) slag with 15 wt% Al<sub>2</sub>O<sub>3</sub> content on the refractory material MgO-C at 1650 °C and low oxygen partial pressure [23,24]. Later on, a porous MgO layer was formed on the sample surface instead of a dense MgO layer. This indicates that under these experimental conditions, Mg gas oxidation from molten oxides is not complete. Such porous MgO layer in industrial and turbulent conditions is not effective for slowing down the slag infiltration into the refractory material. The authors also argued that at temperatures above 1650 °C, the oxidation of MgO-C by atmospheric oxygen or metal oxides in the slag is limited and the main reaction of decarburization of refractory is indirect carbon oxidation in MgO + C. Liu et al. observed direct and indirect dissolution of MgO particles in a low basicity CaO-Al<sub>2</sub>O<sub>3</sub>-SiO<sub>2</sub> slag. He demonstrated that the dissolution rate of MgO increases with increasing slag temperature and decreases strongly with increasing MgO concentration in the slag [25]. Wang et al. investigated the dissolution rate of MgO solids in synthetic ladle slag. According to their experimental results, the increase of Al<sub>2</sub>O<sub>3</sub> and MgO in slag decreases the dissolution rate of MgO due to the formation of magnesia spinel layer at the interface, and the increase of CaO/SiO<sub>2</sub> basicity also increases the dissolution rate of solid MgO in slag [26]. Several studies have demonstrated that when slags containing Al<sub>2</sub>O<sub>3</sub> come into contact with MgO-C refractories, the surface of the refractory forms a protective layer of magnesian spinel. This magnesian spinel layer acts as a barrier, inhibiting the infiltration of slag [27–29].

The present study is a logical continuation of two previous studies, where the effect of SiO<sub>2</sub> addition on changes of thermo-physical properties of slag and the interaction between refining slag with CaO/Al<sub>2</sub>O<sub>3</sub> ratio 1:1 on refractory MgO-C material [7,30]. In this study, the focus was on evaluation of corrosion of MgO-C material with altered CaO/Al<sub>2</sub>O<sub>3</sub> (C/A) ratio in the slag. This study helps to better understand the effect of C/A and SiO<sub>2</sub> in secondary metallurgy slag on refractory corrosion in magnesia-carbon refractory material.

## MATERIALS AND METHODS

The MgO-C samples with 13 wt% of residual carbon based on phenolic resin with adding of Carbores P and 2 wt% of metallic aluminium as an antioxidant, see Table 1. Before the corrosion test, the MgO-C samples catted off from industrial refractory brick with the size 30x30x100 mm. In the upper part of each sample drilled a

25 mm deep hole for installation of Al<sub>2</sub>O<sub>3</sub> holder. After cementing of the Al<sub>2</sub>O<sub>3</sub> holder into sample body, the MgO-C samples were dried 12 hours at 120 °C.

Table 1. The constituent of MgO-C refractory (wt%).

MgO	SiO <sub>2</sub>	CaO	Fe <sub>2</sub> O <sub>3</sub>	Al <sub>2</sub> O <sub>3</sub>	C	Al
97.5	0.6	1.2	0.6	0.1	13	2

The target slags were mixed from industrial slag formers: lime and alumina carrier. The particle size of the slag formers was under 100 µm. All the slags were dried in a desiccator for 24 hours at 120 °C before and after mixing.

According to the CaO/Al<sub>2</sub>O<sub>3</sub> (C/A) ratio the slags can be divided into: High-Al<sub>2</sub>O<sub>3</sub>, Cleanness, and Desulfurization slag, Table 2. C/A ratio is the parameter, determine the task of the secondary metallurgical slag. Slag compositions with C/A-ratio < 1 appear after deep deoxidised steel and steels with high aluminium content. In the case of C/A= 1, the slag has a refining function to agglomerate non-metallic inclusions out of the steel. Slag with C/A > 1 and up to 2 has desulphuration function in steel production processing. The increased MgO content in the High-Al<sub>2</sub>O<sub>3</sub> slag is related to its content in the alumina carrier. Also the Table 2 contains the viscosity values of these three slags at 1650 °C from the previous publication [30].

Table 2. Chemical composition of ladle slags (wt%) and viscosity values (mPa\*s) at 1650 °C.

	High-Al <sub>2</sub> O <sub>3</sub>	Cleanness	Desulfurization
CaO	30.09	43.33	59.77
Al <sub>2</sub> O <sub>3</sub>	53.86	43.33	30.06
SiO <sub>2</sub>	1.05	1.08	0.98
MgO	13.91	11.00	8.12
Fe <sub>2</sub> O <sub>3</sub>	0.99	1.16	0.99
MnO	0.1	0.1	0.08
CaO/Al <sub>2</sub> O <sub>3</sub>	0.56	1.00	1.99
Viscosity (mPa*s)	1777.24	100.29	70.32

The MgO-C corrosion test carried out according to the Finger Testing method, a schematic description of setup is shown in Fig. 1. A pre-dried slag of about 1000 g. melted in a graphite crucible (130 mm height x 80 mm inner diameter) in an induction furnace. After reaching the target temperature, the melt is held for at least 30 minutes at the constant temperature for the homogenization. At the other hand, the MgO-C sample was carbonised in a metal box under graphite powder for 60 minutes at 1000 °C. Right after carbonisation, the MgO-C samples were immersed into the molten slag for 60 minutes.

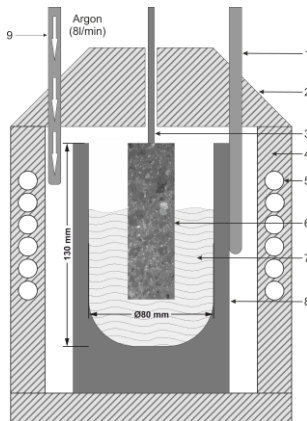


Fig. 1. Induction furnace for finger testing:

- 1-side thermocouple
- 2- ceramic top cover,
- 3- corundum rod,
- 4- furnace,
- 5- induction coil,
- 6- MgO-C sample,
- 7- molten slag,
- 8- graphite crucible
- 9- argon supply

At the end of holding time, the MgO-C samples were removed from the slag and cooled in the air, see Fig. 2. The slag solidified on the sample immediately when the sample left the molten slag,

and forming a dense layer on the MgO-C surface. Afterward, the samples were embedded epoxy resin and cut crosswise to a thickness of 10 millimetres for optical and SEM- analyse.

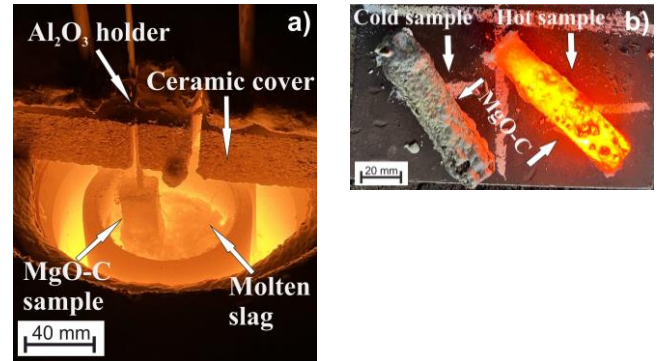


Fig. 2. Finger testing: a) immersion of MgO-C sample in molten slag; b) cooling of samples in the air.

## RESULTS AND DISCUSSION

### Surface analyses of MgO-C

Fig. 3 represents photos of the MgO-C refractory samples immersed in the molten slag at 1650 °C for 60 minutes. After the finger testing experiments, the slag layer was observed to adhere on the surface of the refractories. The thickness of the refractory surface adhered slags was related to wettability of the refractory to the slags, hence, the factors such as the temperature, the roughness, and the porosity of the refractory, and the thermophysical properties of the slags, i.e. surface tension and viscosity of the slag could play an influential role. The present investigation focused on the utilization of a singular type of refractory material as the immersion sample. Consequently, the primary roughness and porosity were assumed to be identical among the specimens. As a result, the depth of corrosion emerged as the determining factor influencing the thickness of the adhered slags. The subsequent analysis considered the influence of viscosity and surface tension on the corrosion process, with specific attention given to the anticipated viscosity value.

The upper part of the refractory material above the slag was oxidised. Compared to the primary MgO-C refractory, the areas that were not in contact with the slag turned from dark to grey. The protective gas employed in the experiments, namely Argon 5.0, contained a minor concentration of oxygen (2-3 ppm oxygen). The oxygen content within the gas initially interacted with the carbon residing on the surface of both the refractory material and the graphite crucible, fostering a reducing atmosphere characterized by the presence of CO gas. Subsequently, the CO gas further reacted with carbon, ultimately yielding CO<sub>2</sub> gas.

Furthermore, a part of the slag was found to be pulled up to the non-immersed part of the refractory to the decarbonised layer. The height of the pulled up liquid slag (h) can be expressed by Jurin's law [31] as depicted in Equation 2. Clearly, the factors such as surface tension, contact angle, and density of the liquid slag could directly affect the h, consequently they also affect the contact area between liquid slags and refractory, namely the corrosion area. The degraded MgO from the side of refractory to the side of liquid slags could change the factors (surface tension, density, and also the contact angle).

$$h = \frac{2\gamma \cos\theta}{\rho g r_0} \quad \text{Equation 2}$$

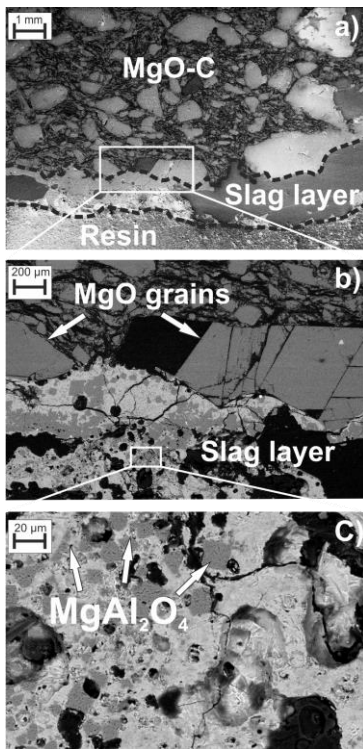
where h is the height of the top of the layer to the liquid surface (m); θ is the contact angle of the liquid on the crucible wall; γ is the surface tension of the liquid (mN·m<sup>-1</sup>); ρ is the density of the liquid (kg·m<sup>-3</sup>); g is the gravitational acceleration and r<sub>0</sub> is the crucible radius (m).



**Fig. 3** Photographs immersed MgO-C refractory in the slag melts: a) High- $\text{Al}_2\text{O}_3$  b) Cleanness, and c) Desulfurization

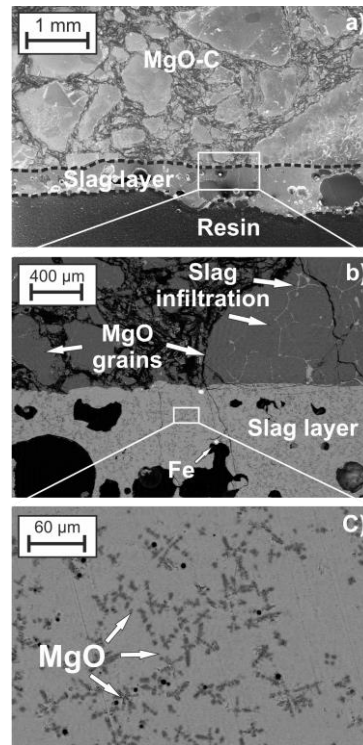
#### Microstructure analyse

Fig. 4 shows the MgO-C sample after contact with the molten High- $\text{Al}_2\text{O}_3$  slag. This slag has a high viscosity of 1777  $\text{mPa}\cdot\text{s}$  at 1650 °C. Because of this high slag viscosity, no visible slag infiltration can be seen. Cracks and ducts in the refractory remain free of slag since the high viscosity of the slag prevents the infiltration of slag into the refractory. Nevertheless, the residual slag build-up on the refractory is up to 2.3 mm.



**Fig. 4.** Cross section of MgO-C after 60 minutes contact with High- $\text{Al}_2\text{O}_3$  slag at 1650 °C.

This is a partially dissolved surface layer of the refractory as well as a cured slag layer on the surface. The slag layer is very dense, which during cooling caused numerous pores and slag cracking. The slag contains high amounts of magnesia spinel, which also increases the risk of slag infiltration into the refractory. The large amount of  $\text{Al}_2\text{O}_3$  in the slag can break up the MgO grains to form more spinel, which makes the infiltration into the refractory even worse. The SEM-EDX analysis found a large amount of magnesia spinel in the slag and on the refractory surface.



**Fig. 5.** Cross section of MgO-C after 60 minutes contact with cleanness slag at 1650 °C.

Fig. 5 shows the refractory material in a cleanness slag. Its viscosity at 1650 °C is seventeen times less (100  $\text{mPa}\cdot\text{s}$ ) than the previous High- $\text{Al}_2\text{O}_3$  slag. These values are sufficient to infiltrate the slag into the refractory material, through the capillaries, and to crack the grains. The total slag layer on the refractory surface was 1.7 mm. Also a massive of the solid particles of MgO in the slag were found. This suggests that the slag in this composition cannot dissolve MgO grains due to its saturation in the slag. Such solid dendrites can be released when the slag is cooled on a hot refractory, when the MgO solubility in the slag decreases as the temperature decreases.

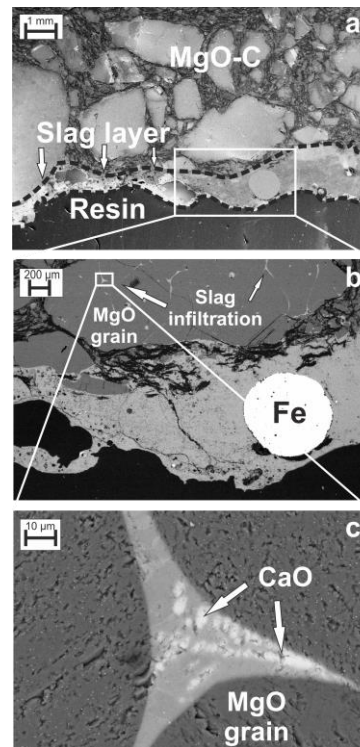


**Fig. 6.** Cross section of MgO-C after 60 minutes contact with desulfurization slag at 1650 °C.

Fig. 6 shows MgO-C after contacting with the desulphurising slag. The depth of the slag layer is 1.57 mm due to the low viscosity 70 $\text{mPa}\cdot\text{s}$  of the slag. In picture b), a spherical reduced iron with a diameter of 0.91 micrometre is observed. Although this slag does not contain more than one percent FeO, it is reduced to pure iron and agglomerated into a single sphere on contact with the refractory carbon. Due to the low viscosity this slag is infiltrated deep into the refractory. Infiltration is more active in areas where there is no carbon. These are often splits in the MgO grains, where the slag is infiltrated by the droplet effect. As the slag contains a large amount of CaO, its maximum allowable solubility in the slag drops and it is isolated separately as CaO solid.

## CONCLUSIONS

In present work, the effect of different slags on the MgO-C refractory was investigated. The different C/A-ratio in the slag affected the capability of the slag to dissolve the MgO-grain, and prevented slag infiltration into the refractory:

1. Slag infiltration into the MgO-C refractory was not detected at a viscosity of more than 100 mPa\*s.
2. Although high-Al<sub>2</sub>O<sub>3</sub> was reacted with the refractory, it could dissolve the MgO grains to form MgAl<sub>2</sub>O<sub>4</sub>.
3. Cleaness slag has low viscosity values, which lead them infiltrate deeper into the MgO-C refractory. At the same time, dissolution of MgO grains was not possible due to their saturation in the slag.
4. The desulphurized slag has the lowest viscosity index, because of its infiltration into the refractory the deepest. Solid CaO is released from the solidified slag as it is saturated with it.

## REFERENCES

- [1] X. Wei, E. Storti, S. Dudczig, A. Yehorov, O. Fabrichnaya, C.G. Aneziris, O. Volkova, The interaction of carbon-bonded ceramics with Arco iron, *J. Eur. Ceram. Soc.* (2022). <https://doi.org/10.1016/j.jeurceramsoc.2022.04.058>.
- [2] S. Jansson, V. Brabie, P. Jönsson, Corrosion mechanism of commercial MgO-C refractories in contact with different gas atmospheres, *ISIJ Int.* 48 (2008) 760–767. <https://doi.org/10.2355/isijinternational.48.760>.
- [3] H. Zielke, T. Wetzig, C. Himcinschi, M. Abendroth, M. Kuna, C.G. Aneziris, Influence of carbon content and coking temperature on the biaxial flexural strength of carbon-bonded alumina at elevated temperatures, *Carbon N. Y.* 159 (2020) 324–332. <https://doi.org/10.1016/j.carbon.2019.12.042>.
- [4] J. Poirier, A review: Influence of refractories on steel quality, *Metall. Res. Technol.* 112 (2015). <https://doi.org/10.1051/met/2015028>.
- [5] Z. Liu, J. Yu, X. Yang, E. Jin, L. Yuan, Oxidation resistance and wetting behavior of MgO-C refractories: Effect of carbon content, *Materials (Basel)*. 11 (2018). <https://doi.org/10.3390/ma11060883>.
- [6] W. da Silveira, G. Falk, Production of MgO-X Refractory Material with Cellular Matrix by Colloidal Processing, *Low Carbon Econ.* 03 (2012) 83–91. <https://doi.org/10.4236/lce.2012.323012>.
- [7] A. Yehorov, G. Ma, O. Volkova, Interaction between MgO-C bricks and ladle slag with a 1:1 CaO/Al<sub>2</sub>O<sub>3</sub> ratio and varying SiO<sub>2</sub> content, *Ceram. Int.* 47 (2021) 11677–11686. <https://doi.org/10.1016/j.ceramint.2021.01.007>.
- [8] S.K. Sadrnezhad, Z.A. Nemati, S. Mahshid, S. Hosseini, B. Hashemi, Effect of Al antioxidant on the rate of oxidation of carbon in MgO-C refractory, *J. Am. Ceram. Soc.* 90 (2007) 509–515. <https://doi.org/10.1111/j.1551-2916.2006.01391.x>.
- [9] R. Sarkar, *Refractory Technology*, 2016. <https://doi.org/10.1201/9781315368054>.
- [10] E.M.M. Ewais, Carbon based refractories, *J. Ceram. Soc. Japan*. 112 (2004) 517–532. <https://doi.org/10.2109/jcersj.112.517>.
- [11] T. Bahtli, D.Y. Hopa, V.M. Bostanci, N.S. Ulvan, S.Y. Yasti, Corrosion behaviours of MgO-C refractories: Incorporation of graphite or pyrolytic carbon black as a carbon source, *Ceram. Int.* 44 (2018) 6780–6785. <https://doi.org/10.1016/j.ceramint.2018.01.097>.
- [12] D.A. Brosnan, *Corrosion of refractories*, 2004. <https://www.jurispro.com/files/documents/doc-1066205184-article-1609.pdf>.
- [13] T.L. Dhami, O.P. Bahl, B.R. Awasthy, Oxidation-resistant carbon-carbon composites up to 1700 °C, *Carbon N. Y.* 33 (1995) 479–490. [https://doi.org/10.1016/0008-6223\(94\)00173-W](https://doi.org/10.1016/0008-6223(94)00173-W).
- [14] B. yue Ma, X. ming Ren, Z. Gao, F. Qian, Z. yang Liu, G. qi Liu, J. kun Yu, G. feng Fu, Influence of pre-synthesized Al<sub>2</sub>O<sub>3</sub>-SiC composite powder from clay on properties of low-carbon MgO-C refractories, *J. Iron Steel Res. Int.* 29 (2022) 1080–1088. <https://doi.org/10.1007/s42243-021-00653-8>.
- [15] M.A. Faghihi-Sani, A. Yamaguchi, Oxidation kinetics of MgO-C refractory bricks, *Ceram. Int.* 28 (2002) 835–839. [https://doi.org/10.1016/S0272-8842\(02\)00049-4](https://doi.org/10.1016/S0272-8842(02)00049-4).
- [16] S.K. Sadrnezhad, S. Mahshid, B. Hashemi, Z.A. Nemati, Oxidation mechanism of C in MgO-C refractory bricks, *J. Am. Ceram. Soc.* 89 (2006) 1308–1316. <https://doi.org/10.1111/j.1551-2916.2005.00863.x>.
- [17] S. Nanda, A. Choudhury, K.S. Chandra, D. Sarkar, Raw materials, microstructure, and properties of MgO-C refractories: Directions for refractory recipe development, *J. Eur. Ceram. Soc.* 43 (2023) 14–36. <https://doi.org/10.1016/j.jeurceramsoc.2022.09.032>.
- [18] W.E. Lee, S. Zhang, Melt corrosion of oxide and oxide-carbon refractories, *Int. Mater. Rev.* 44 (1999) 77–104. <https://doi.org/10.1179/095066099101528234>.
- [19] S. Jansson, V. Brabie, P. Jonsson, Corrosion mechanism and kinetic behaviour of MgO-C refractory material in contact with CaO-Al<sub>2</sub>O<sub>3</sub>-SiO<sub>2</sub>-MgO slag, *Scand. J. Metall.* 34 (2005) 283–292. <https://doi.org/10.1111/j.1600-0692.2005.00748.x>.
- [20] S.N. Silva, F. Vernilli, S.M. Justus, O.R. Marques, A. Mazine, J.B. Baldo, E. Longo, J.A. Varela, Wear mechanism for blast furnace hearth refractory lining, *Ironmak. Steelmak.* 32 (2005) 459–467. <https://doi.org/10.1179/174328105X48160>.
- [21] W. Huihua, W. Channa, X. Yingjun, J. Kun, Q. Tianpeng, T. Jun, W. Deyong, Induced Electro-Deposition of High Melting-Point Phases on MgO-C Refractory in CaO-Al<sub>2</sub>O<sub>3</sub>-SiO<sub>2</sub>-(MgO) Slag at 1773 K, *High Temp. Mater. Process.* 38 (2019) 396–403. <https://doi.org/10.1515/htmp-2018-0035>.
- [22] R.A.A. Borges, G.F.B. Lenz e Silva, A statistical and post-mortem study of wear and performance of MgO-C resin bonded refractories used on the slag line ladle of a basic oxygen steelmaking plant, *Eng. Fail. Anal.* 78 (2017) 161–168. <https://doi.org/10.1016/j.engfailanal.2017.03.020>.
- [23] M. Guo, S. Parada, P.T. Jones, J. Van Dyck, E. Boydens, D. Durinck, B. Blanpain, P. Wollants, Degradation mechanisms of magnesia-carbon refractories by high-alumina stainless steel slags under vacuum, *Ceram. Int.* 33 (2007) 1007–1018. <https://doi.org/10.1016/j.ceramint.2006.03.009>.
- [24] M. Guo, S. Parada, P.T. Jones, E. Boydens, J. V. Dyck, B. Blanpain, P. Wollants, Interaction of Al<sub>2</sub>O<sub>3</sub>-rich slag with MgO-C refractories during VOD refining-MgO and spinel layer formation at the slag/refractory interface, *J. Eur. Ceram. Soc.* 29 (2009) 1053–1060. <https://doi.org/10.1016/j.jeurceramsoc.2008.07.063>.
- [25] J. Liu, M. Guo, P.T. Jones, F. Verhaeghe, B. Blanpain, P. Wollants, In situ observation of the direct and indirect dissolution of MgO particles in CaO-Al<sub>2</sub>O<sub>3</sub>-SiO<sub>2</sub>-based slags, *J. Eur. Ceram. Soc.* 27 (2007) 1961–1972. <https://doi.org/10.1016/j.jeurceramsoc.2006.05.107>.
- [26] D. Wang, X. Li, H. Wang, Y. Mi, M. Jiang, Y. Zhang, Dissolution rate and mechanism of solid MgO particles in synthetic ladle slags, *J. Non. Cryst. Solids*. 358 (2012) 1196–1201. <https://doi.org/10.1016/j.jnoncrysol.2012.02.014>.
- [27] X. ming Ren, B. yue Ma, S. ming Li, H. xia Li, G. qi Liu, W. gang Yang, F. Qian, S. xian Zhao, J. kun Yu, Comparison study of slag corrosion resistance of MgO-MgAl<sub>2</sub>O<sub>4</sub>, MgO-CaO and MgO-C refractories under electromagnetic field, *J. Iron Steel Res. Int.* 28 (2021) 38–45. <https://doi.org/10.1007/s42243-020-00421-0>.
- [28] M. Yan, Y. Li, H. Li, Y. Sun, H. Qin, Q. Zheng, Preparation and ladle slag resistance mechanism of MgAlON bonded Al<sub>2</sub>O<sub>3</sub>-MgAlON-Zr<sub>2</sub>Al<sub>3</sub>C<sub>4</sub>-(Al<sub>2</sub>CO)<sub>1-x</sub>(AlN)<sub>x</sub> refractories, *Ceram. Int.* 45 (2019) 346–353. <https://doi.org/10.1016/j.ceramint.2018.09.173>.
- [29] T. Preisker, P. Gehre, G. Schmidt, C.G. Aneziris, C. Wöhrmeyer, C. Parr, Kinetics of the formation of protective slag layers on MgO-MgAl<sub>2</sub>O<sub>4</sub>-C ladle bricks determined in laboratory, *Ceram. Int.* 46 (2020) 452–459. <https://doi.org/10.1016/j.ceramint.2019.08.282>.
- [30] A. Yehorov, X. Wei, M.R. Bellé, O. Volkova, Influence of SiO<sub>2</sub> -adding on the thermophysical properties and crystallization behaviour of ladle slags, *Steel Res. Int.* (2023). <https://doi.org/10.1002/srin.202300173>.
- [31] T. Shyrokykh, X. Wei, S. Seetharaman, O. Volkova, Vaporization of Vanadium Pentoxide from CaO-SiO<sub>2</sub>-VO<sub>x</sub> Slags During Alumina Dissolution, *Metall. Mater. Trans. B.* 52 (2021) 1472–1483. <https://doi.org/10.1007/s11663-021-02114-9>.